Measuring coupled oscillations using an automated video analysis technique based on image recognition

2005 Eur. J. Phys. 26 1149

(http://iopscience.iop.org/0143-0807/26/6/023)

INSTITUTE OF PHYSICS PUBLISHING EUROPEAN JOURNAL OF PHYSICS

Eur. J. Phys. **26** (2005) 1149–1155 doi:10.1088/0143-0807/26/6/023

Measuring coupled oscillations using an automated video analysis technique based on image recognition

Juan A Monsoriu, Marcos H Giménez, Jaime Riera and Ana Vidaurre

Departamento de Física Aplicada, Universidad Politécnica de Valencia, E-46022 Valencia, Spain

E-mail: jmonsori@fis.upv.es

Received 21 May 2005, in final form 4 August 2005
Published 28 September 2005
Online at stacks.iop.org/EJP/26/1149

Abstract

The applications of the digital video image to the investigation of physical phenomena have increased enormously in recent years. The advances in computer technology and image recognition techniques allow the analysis of more complex problems. In this work, we study the movement of a damped coupled oscillation system. The motion is considered as a linear combination of two normal modes, i.e. the symmetric and antisymmetric modes. The image of the experiment is recorded with a video camera and analysed by means of software developed in our laboratory. The results show a very good agreement with the theory.

1. Introduction

Digital techniques have proved to be a very useful tool for the analysis and understanding of physical concepts [1–4]. In particular, digital simulations allow the visualization of the physical process. In this way, the students can improve their knowledge of the real physical process through a model rather than through its oral explanation [5–7]. Unfortunately, many simulations used in teaching physics only display the end product but not contribute to the understanding of the physical phenomena. When using simulations the teacher must be sure that they serve to increase the students' understanding [8].

Video analysis was initially used to investigate simple problems related to kinematic concepts [9, 10]. The development of point-and-click tools such as VideoPoint™ and VideoGraph™ allows the quantitative analysis of more complex problems [11, 12]. Recent works [13, 14] confirm the interest in video analysis applied to more advanced concepts in physics. It has also been proposed as a remote and non-invasive technique in the area of

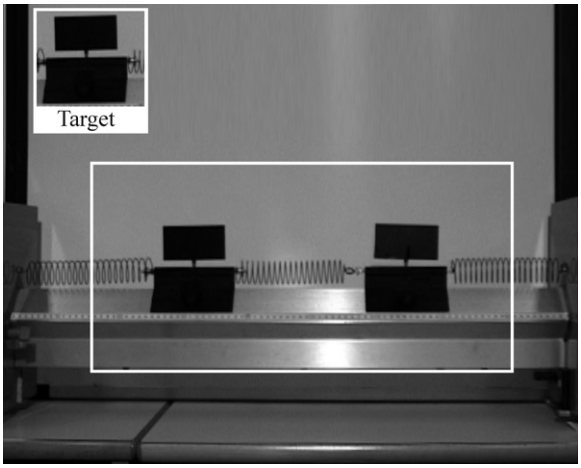

Figure 1. Experimental arrangement, where the detection windows has been framed. The object to be detected is shown in the upper-right corner.

system identification involving nonlinear characteristics of mechanical and structural systems [15].

However, the application of video analysis to the investigation of increasingly complex problems involves working with a great number of images. In order to reduce errors and avoid the excessively tedious process of image processing, new automatic image recognition techniques have been developed [15, 16]. In this work, we analyse a mechanical system consisting of two gliders mounted on an air track. Both gliders are connected to each other by a spring and to the fixed extreme of the air track by similar springs. Therefore, the system consists of two coupled oscillators. Recently, a simple method for observing normal modes in coupled oscillators has been proposed [17]. This method consists of applying a frequency-dependent force to the system and using resonance to excite each mode separately. However, it does not allow the analysis of a coupled movement generated by an arbitrary combination of the two normal modes. The latter case can be studied using the video analysis technique that gives the position of both gliders every 0.04 s. With this technique, the student not only obtains quantitative results, but thanks to the visual display of the process he/she also gains a better understanding of the physical phenomenon. We have used standard linear correlation [18] as the basis for the detection technique. It is the same technique as that used to analyse the movement of a body at constant speed and constant acceleration [16]. In this case, the positions of more than one object on each image need to be obtained. The detection technique has also been shown to be suitable for this task, opening a new field of applications.

This paper is organized as follows. The experimental design and the measurement techniques are shown in section 2. The theoretical basis of a system of coupled oscillators is described in section 3. The experimental results, fitting and discussion are explained in section 4. Finally, concluding remarks are presented in section 5.

2. Experimental procedure

The experimental arrangement consists of two identical gliders connected to each other by a spring and to the confining walls by two other identical springs. The gliders are mounted on an air track in which friction can be regulated through the air flow (see figure 1).

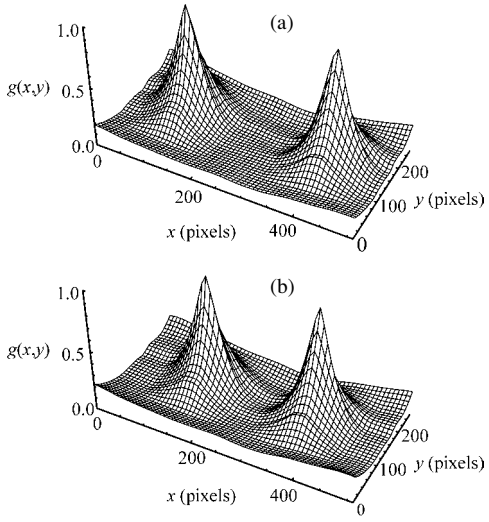

Figure 2. The correlation function between the input scene and the objects to be detected, when the distance between the gliders is (a) maximum and (b) minimum. The axes x and y represent the pixel position in the detection window.

The digital camera used in the experiments was a Panasonic NV-DS15EG, with an exposure time of 1/2000 s and a rate of 25 frames s^{-1} providing a time resolution of 0.04 s. The camera was placed with its axis perpendicular to the movement direction, at a distance of 1.5 m. The video system was PAL (phase alternation by line) that produces 720 × 576 pixel images. We performed the analysis on 512 × 256 pixel windows, thus obtaining a good balance between information accuracy and computational cost.

For the localization of the moving objects, we considered each frame as an input scene, $f(x, y)$, and used a detached image as the filter for the particular object of interest, $h(x, y)$. The correlation function between these functions is given by [16, 18]

$$g(x, y) = \int_{-\infty}^{\infty}\int_{-\infty}^{\infty} f(x', y')h(x' - x, y' - y)\,\mathrm{d}x'\,\mathrm{d}y'. \tag{1}$$

The maximum of the correlation function (see figure 2) corresponds to the location where the scene is most similar to the target object.

When working with digitized images, the correlation function involves double integrations that require much computation time. However, the process can be substantially simplified by using the properties of Fourier transforms. It can be easily proved that [19]

$$\mathrm{g}(x, y) = F^{-1}\{F\{f(x, y)\}F\{h(-x, -y)\}\}. \tag{2}$$

In this way, the correlation function can be calculated relatively rapidly using the direct and inverse Fourier transforms based on fast Fourier transform (FFT) algorithms. The image recognition software has been developed in Visual Basic and runs on Windows platforms. Two extreme positions of the gliders were tested in order to know if the system resolution allows the location of both gliders. Figure 2 shows the correlation function at these positions, where the distance between the gliders is maximum (figure 2(a)) and minimum (figure 2(b)). In all cases, the system resolution allowed the location of both gliders.

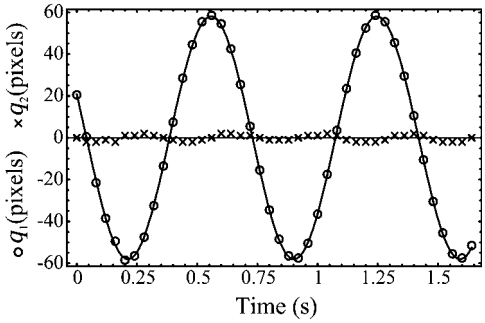

Figure 3. Plots of normal coordinates q_1 and q_2 versus time when the initial conditions favour the symmetric mode.

3. Theoretical basis

Let us consider the system shown in figure 1 consisting of two equal masses m connected to each other by a spring with elastic constant k_i, and to a fixed point by similar springs with elastic constant k_0. The system is horizontally aligned; let us now consider a one-dimensional motion along the line connecting the masses. We define the coordinates, x_1 and x_2, as the displacement to the right from the equilibrium for gliders 1 and 2, respectively. If we apply Newton's law to each mass, we find the following equations of motion:

$$m\ddot{x}_1 = -k_0 x_1 - k_i(x_1 - x_2) - c\dot{x}_1 \tag{3a}$$

$$m\ddot{x}_2 = -k_0 x_2 - k_i(x_2 - x_1) - c\dot{x}_2 \tag{3b}$$

where c is the coefficient of the velocity-dependent damping force. It is possible to uncouple these equations by introducing a new set of coordinates $q_1 = (x_2 + x_1)$ and $q_2 = (x_2 - x_1)$. Then

$$m\ddot{q}_1 + c\dot{q}_1 + k_0 q_1 = 0 \tag{4a}$$

$$m\ddot{q}_2 + c\dot{q}_2 + (2k_i + k_0)q_2 = 0 \tag{4b}$$

Each of the two independent equations corresponds to the motion of a damped harmonic oscillator. The solution of these equations is

$$q_1 = A_1\, \mathrm{e}^{-t/\tau} \sin(\omega_1 t + \phi_1) \tag{5a}$$

$$q_2 = A_2\, \mathrm{e}^{-t/\tau} \sin(\omega_2 t + \phi_2) \tag{5b}$$

where $\omega_1 = \sqrt{\omega_{01}^2 - \gamma^2}$ and $\omega_2 = \sqrt{\omega_{02}^2 - \gamma^2}$ are the angular frequencies corresponding to each normal mode; ϕ_1 and ϕ_2 represent the initial phase of each oscillating mode, $\tau = \gamma^{-1}$ is the relaxation time and $\gamma = c/(2m)$ is the damping coefficient. If this coefficient is negligible, the angular frequencies are $\omega_{01} = \sqrt{\frac{k_0}{m}}$ and $\omega_{02} = \sqrt{\frac{(2k_i + k_0)}{m}}$.

4. Results and discussion

4.1. Normal modes

First, we tried to reproduce the oscillating normal modes separately. To this end, the system was excited in the appropriate way. In figure 3 the coordinates q_1 and q_2 are plotted as a

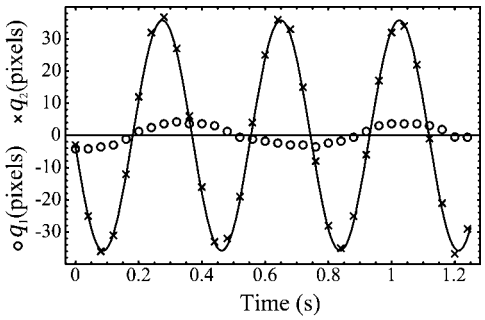

Figure 4. Plots of normal coordinates q_1 and q_2 versus time when the initial conditions favour the antisymmetric mode.

function of time. Hereafter, the corresponding uncertainty bars of the data are not shown in this kind of representation because they have the same size of symbol. Observe in figure 3 that the antisymmetric mode is almost negligible. This is because the initial displacement of the masses ($x_{01} = 2$ cm, $x_{02} = 2$ cm) is the same, and this favours the symmetric mode in which both masses move in the same direction. From the fitting of the curve we obtain $A_1 = 58.0(0.4)$ pixels, $\omega_{01} = 9.11(0.02)$ rad s^{-1} and $\phi_1 = -3.51(0.02)$ rad where the number in parenthesis is the numerical value of the combined standard uncertainty expressed in the same unit of the quoted result. The parameters and their uncertainties were obtained using the standard least-squares method.

Figure 4 shows the corresponding results when the initial displacements favour the antisymmetric mode ($x_{01} = -2$ cm, $x_{02} = 2$ cm). In this case, the difference in the presence of both modes is not so remarkable as in the previous situation, perhaps due to noise effects. From the fitting of the experimental data we obtain $A_2 = 35.6(0.4)$ pixels, $\omega_{02} = 16.86(0.04)$ rad s^{-1} and $\phi_2 = -3.04(0.02)$ rad. The theoretical relationship between the angular frequencies of the normal modes obtained from the elastic constants of the system, $k_i = 55.3(0.9)$ N m^{-1} and $k_0 = 45.9(0.6)$ N m^{-1}, is $\frac{\omega_{02}}{\omega_{01}} = \sqrt{1 + 2\frac{k_i}{k_0}} = 1.846(0.046)$. This result is in a very good agreement with the value obtained in the video analysis, $\left.\frac{\omega_{02}}{\omega_{01}}\right|_{\text{exp}} = 1.851(0.006)$. In both cases, the value of the combined standard uncertainty has been determined through the law of propagation of uncertainty [20].

4.2. Movement without friction

If the air flow of the air track is high enough, the damping coefficient is very small. Figure 5 shows the normal modes in the case of the negligible damping coefficient, the initial position of the masses being $x_{01} = 4$ cm and $x_{02} = 2$ cm. From the fitting of both curves we obtain $A_1 = 41.7(0.3)$ pixels, $\omega_{01} = 9.14(0.02)$ rad s^{-1} and $\phi_1 = -0.91(0.02)$ rad for the symmetric mode, and $A_2 = 13.8(0.3)$ pixels, $\omega_{02} = 16.93(0.04)$ rad s^{-1} and $\phi_2 = -0.49(0.04)$ for the antisymmetric mode. As can be seen, the values of ω_{01} and ω_{02} are in very good agreement with the frequencies of the two independent normal modes obtained in section 4.1.

4.3. Damped movement

By reducing the air flow of the air track we have a damped coupled oscillating system. Figure 6 shows the normal modes when the initial positions of the masses are $x_{01} = 4$ cm and $x_{02} = 2$ cm. From the fitting of both curves we obtain $A_1 = 28.5(0.6)$ pixels, $\omega_1 = 9.04(0.02)$ rad s^{-1}

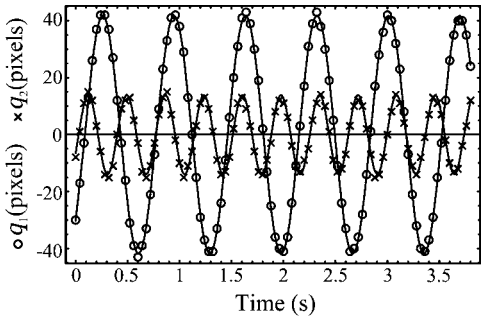

Figure 5. Plots of normal coordinates q_1 and q_2 versus time when there are no friction forces.

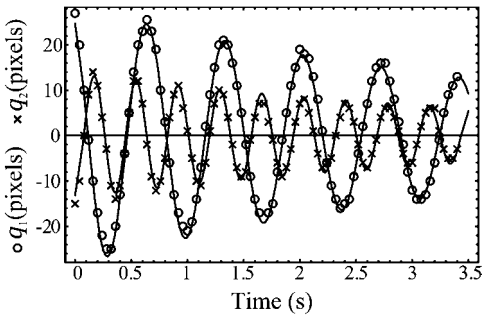

Figure 6. Plots of normal coordinates q_1 and q_2 versus time when damping friction forces are present.

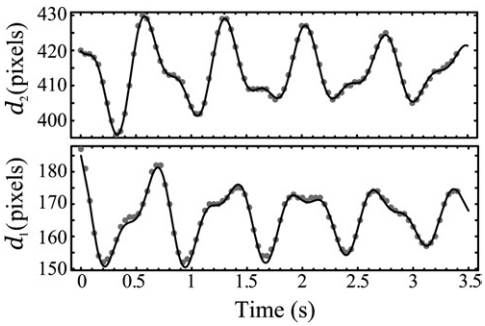

Figure 7. Position of each mass (d_1, d_2) versus time and the theoretical prediction corresponding to linear combination from the normal modes. Taking the origin in the lower left corner of the window shown in figure 1, each mass is located in $d_1 = 166 + x_1$ and $d_2 = 414 + x_2$, respectively.

and $\phi_1 = 2.09(0.03)$ rad for the symmetric mode, and $A_2 = 13.6(0.5)$ pixels, $\omega_2 = 16.84(0.04)$ rad s^{-1} and $\phi_2 = -1.31(0.06)$ rad for the antisymmetric mode. The relaxation time is $\tau = 4.3(0.2)$ s. These results agree with the theoretical predictions, as can be seen in figure 7; this figure represents the position of each mass as a function of time and the corresponding linear combination of the normal modes.

5. Concluding remarks

Video analysis and a simple image recognition technique have proved to be a useful method for analysing damped coupled oscillators. Furthermore, the possibility of following the movement frame by frame opens new ways for the understanding of complex physical processes. This technique increases the pedagogical efficiency as compared to traditional methods that require more sophisticated explanation to reach similar results.

Acknowledgments

This work has received financial support by the Universidad Politécnica de Valencia (PII 20020632), Spain. We would like to thank the R+D+I Linguistic Assistance Office at the Universidad Politécnica de Valencia for their help in revising this paper.

References

[1] Fuller R and Zollman D 1995 *Physics InfoMall* (Armonk, NY: The Learning Team)
[2] Brasell H 1987 The effect of real-time laboratory graphing on learning graphic representations of distance and velocity *J. Res. Sci. Teach.* **24** 385–95
[3] Vidaurre A, Riera J, Giménez M H and Monsoriu J A 2002 Contribution of digital simulation in visualizing physics processes *Comput. Appl. Eng. Educ.* **10** 45–9
[4] Riera J, Giménez M H, Vidaurre A and Monsoriu J A 2002 Digital simulation of wave motion *Comput. Appl. Eng. Educ.* **10** 161–6
[5] Escalada L T and Zollman D A 1997 An investigation on the effects of using interactive digital video in a physics classroom on student learning and attitudes *J. Res. Sci. Teach.* **34** 467–89
[6] Shin Y S 2002 Virtual reality simulations in web-based science education *Comput. Appl. Eng. Educ.* **10** 18–45
[7] Cadmus R R 1990 A video technique to facilitate the visualization of physical phenomena *Am. J. Phys.* **58** 397–9
[8] Steinberg R N 2000 Computer in teaching science: to simulate or not to simulate? *Phys. Educ. Res., Am. J. Phys. Suppl.* **68** S37–41
[9] Zollman D A, Noble M L and Curtin R 1987 Modeling the motion of an athlete: an interactive video lesson for teaching physics *J. Educ. Technol. Syst.* **15** 249–57
[10] Laws P W 1991 Calculus-based physics without lectures *Phys. Today* **24** 24–31
[11] Wehrbein W M 2001 Using video analysis to investigate intermediate concepts in classical mechanics *Am. J. Phys.* **69** 818–20
[12] Salumbides E J, Maristela J, Uy A and Karremans K 2002 A vision-based motion sensor for undergraduate laboratories *Am. J. Phys.* **70** 868–71
[13] Cross R 2002 Measurements of the horizontal coefficient of restitution for a superball and a tennis ball *Am. J. Phys.* **70** 482–9
[14] Greczylo T and Debowska E 2002 Using a digital video camera to examine coupled oscillations *Eur. J. Phys.* **23** 441–7
[15] Chung H-C, Liang J, Kushiyama S and Shinozuka M 2004 Digital image processing for non-linear system identification *Int. J. Non-Linear Mech.* **39** 691–707
[16] Riera J, Monsoriu J A, Giménez M H, Hueso J L and Torregrosa J A 2003 Using image recognition to automate video analysis of physical processes *Am. J. Phys.* **71** 1075–9
[17] Givens R, Bonfim O F A and Ormond R B 2003 Direct observation of normal modes in coupled oscillators *Am. J. Phys.* **71** 87–90
[18] VanderLugt A 1964 Signal detection by complex spatial filtering *IEEE Trans. Inf. Theory* **10** 39–145
[19] Gaskill J D 1978 *Linear Systems, Fourier Transforms and Optics* (New York: Wiley) pp 196
[20] 1995 *Guide to the Expression of Uncertainty in Measurement* (Switzerland: ISO)